BPB Reports

Regular Article

Two Modes of Toxicity of Lipid Nanoparticles Containing a pH-Sensitive Cationic Lipid on Human A375 and A375-SM Melanoma Cell Lines

Ahmed Y. AlBaloul,[a] Yusuke Sato,[a,*] Nako Maishi,[b] Kyoko Hida,[b] and Hideyoshi Harashima[a,*]

[a]*Laboratory for Molecular Design of Pharmaceutics, Faculty of Pharmaceutical Sciences, Hokkaido University, Kita-12, Nishi-6, Kita-Ku, Sapporo 060–0812, Japan;* [b]*Vascular Biology and Molecular Pathology, Graduate School of Dental Medicine, Hokkaido University, Kita-13, Nishi-7, Kita-Ku, Sapporo 060–8586, Japan*
Received May 10, 2019; Accepted August 2, 2019

Melanomas are one of the most aggressive form of skin cancer and are resistant to many cancer therapies. Lipid nanoparticles (LNPs) containing a pH-sensitive cationic lipid, YSK05 (YSK05-LNPs), for delivering short interfering RNA (siRNA) were found to strongly triggers *in vitro* toxicity in human A375 and A375-SM melanoma cell lines regardless of gene silencing. Assessing the localization of the toxicity was done by controlling the cellular uptake of the YSK05-LNPs that contained different polyethyleneglycol (PEG)-lipid. The YSK05-LNPs exhibited consistent dose- and time-dependent toxicity, independent of their cellular uptake, indicating that the toxicity is triggered by an interaction between the YSK05-LNPs and the cell surface. Treatment with free YSK05 resulted in only time-dependent toxicity. These results suggest that the YSK05-LNPs trigger two modes of action; a fast-acting component that is related to the LNP formulation and a slow-acting mode, which is related to the YSK05 lipid itself. Necrosis was determined to be the cause of cell death, as evidenced by the results of Annexin V assays, which are specific for confirming lipid-based toxicity. These findings indicate that these YSK05-LNPs have substantial potential for use as an antimelanoma agent as both an RNA interference-based drug and as a chemotherapeutic drug.

Key words lipid nanoparticles, melanoma, nanotoxicity, pH-sensitive cationic lipid, anticancer, necrosis

INTRODUCTION

Melanomas, which account for approximately 1% of skin malignant tumors, arise from the occurrence of several genetic mutations in melanocytes.[1)] Melanomas represents the most aggressive form of skin cancer and once they become metastatic, patients usually have a very poor prognosis with an overall median survival of only 6 to 9 months.[2)] The available treatments for melanoma patients include surgery, radiation therapy, chemotherapy, immunotherapy, and targeted therapy. However, emerging drug resistance and systemic toxicity restrict the efficacy of these treatments, despite the ongoing progress in the treatment of metastatic melanomas.[3)]

Because genetic mutations are responsible for the drug resistant of this type of cancer, RNA interference (RNAi)-mediated specific silencing of mutated genes by short interfering RNA (siRNA) would be a promising approach for the treatment of metastatic melanomas. Nanoparticles are useful for overcoming the rapid clearance, poor stability and biodistribution of siRNAs due to their unique physicochemical properties including low molecular weight, hydrophilicity and negative charges.[4)]

Lipid nanoparticles (LNP) are one of the most advanced platforms for delivering siRNA *in vivo*. Recent many efforts in developing potent cationic lipids have dramatically improved the efficiency of delivery of siRNAs *in vivo*, resulting in the approval of the first-ever LNP-based RNAi medicine, ONPATTRO™, in 2018.[5)] We, in previous studies, reported on the development of an original cationic lipid, YSK05, and demonstrated its gene silencing activity in multiple target tissues and cells, including the liver, brain, immune cells, and tumors.[6–10)]

In the present study, we applied YSK05-containing LNPs (YSK05-LNPs) to the treatment of human metastatic melanoma cell lines, A375 and A375-SM which are super-metastatic strains obtained from A375 after three lung colonization cycles.[11,12)] To our surprise, the YSK05-LNPs strongly induced cell death in both cell lines and this was not dependent on the cellular uptake of the particles or the siRNAs. The free form of YSK05 also induced cell death. These findings suggested that YSK05 can function as both an enhancer for siRNA delivery and a chemotherapeutic drug against metastatic melanoma.

MATERIALS AND METHODS

Materials The pH-sensitive cationic lipid, YSK05 were synthesized as described previously.[8)] Cholesterol (chol) was purchased from SIGMA Aldrich (St. Louis, MO). 1,2-Dimirystoyl-*sn*-glycero methoxyethyleneglycol 2000 ether (PEG-DMG) and 1,2-distearoyl-*sn*-glycerol methoxyethyleneglycol 2000 ether (PEG-DSG) were obtained from NOF Corporation (Tokyo, Japan). 1,1'-Dioctadecyl-3,3,3'3'-tetramethylindocarbocyanine (DiD) was purchased from Molecular Probes (Eugene, OR, USA). Melanoma A375 cells were purchased from the American Type Culture Collection (ATCC).

*To whom correspondence should be addressed. e-mail: y_sato@pharm.hokudai.ac.jp; harasima@pharm.hokudai.ac.jp

A375SM cells were generously provided by Dr. Fidler (M.D. Anderson Cancer Centre, Houston, TX, USA). Minimum essential media (MEM), penicillin-streptomycin (P/S), and trypsin were obtained from Gibco (Tokyo, Japan). Fetal bovine serum (FBS) and *tertiary*-butyl alcohol (*tert*-BuOH) were purchased from Wako Chemicals (Osaka, Japan). Ethylene diamine tetraacetic acid (EDTA) and cell counting kit-8 (CCK8) were purchased from Dojindo Molecular Technologies (Tokyo, Japan). MEBCYTO® apoptosis kit (Annexin V-FITC Kit) was obtained from Medical and Biological Laboratories CO., LTD (Nagoya, Japan). Anti-GL4 siRNA (siGL4, sense: 5'-CCG UCG UAU UCG UGA GCA AdTdT-3'; antisense: 5'-UUG CUC ACG AAU ACG ACG GdTdT-3') was purchased from Hokkaido System Science Co., Ltd. (Sapporo, Japan).

Preparation of LNPs LNPs were prepared using the *tert*-BuOH dilution method as described previously.[8] Four hundred microliters of a 90% *tert*-BuOH solution containing YSK05, cholesterol (chol), PEG-lipid at a molar ratio of 70/30/3 were prepared at a concentration of 7.5 mM total lipid. For the cellular uptake experiment, 0.05 mol% of DiD was added to the above solution. The lipid solution was mixed with 200 μL of a 0.4 mg/mL siRNA. The mixture was collected in a 1 mL syringe with a 27-gauge needle and injected into a conical tube containing 2 mL of 20 mM citrate buffer (pH 4.0) under vigorous mixing. The resulting LNP solution was diluted with 3.5 mL of D-PBS(-) and transferred into an Amicon Ultra-15 centrifugal filter tube (MWCO 100 kDa, Millipore). The LNP solution were further diluted with 10.5 mL of D-PBS(-). Two rounds of centrifugation were performed at 1000 g and 25°C for 21 to 23 min. After centrifugation, the retentate was made up to 1000 μL with D-PBS(-) and stored at 4°C. Particle size was measured using a Zetasizer Nano ZS ZEN 3600 (Marven Instruments, Worcestershire, UK).

Cell Culture Cells were cultured in cell-culture dishes (Corning) containing MEM supplemented with 10% FBS, penicillin (100 U/mL) and streptomycin (100 μg/mL) at 37°C in 5% CO_2. Subculturing was performed at a density of 2×10^5 cells after reaching a confluency of 60 to 80% by using PBS(-) containing 0.25% trypsin and 0.02% EDTA as a detaching buffer.

WST-8 Cell Viability Assay Cells were seeded at a density of 1×10^4 cells per well in 48-well plates in 300 μL of growth media. Twenty-four hours after seeding, the media was removed by aspiration and cells were exposed to the LNPs or free YSK05 at the indicated final lipid concentration. The free YSK05 dissolved in *tert*-BuOH (128 mM) was diluted with growth media to produce the final YSK05 concentration. The final concentration of *tert*-BuOH was fixed at 0.25 v/v% where negligible toxicity was observed (Fig. S1). Cell viability was measured at 24, 48, and 72 h after the exposure using a CCK-8 (Cell Counting Kit-8, Dojindo Molecular Technologies, Japan). Ten microliters of CCK-8 solution was added to each well, which were then incubated for 1 to 2 h at 37°C in 5% CO_2. Absorbance was measured at 450 nm using a spectrofluorometer (Enspire, PerkinElmer, MA, USA). All experiments were done in duplicates.

Measurement of Cellular Uptake Cells were seeded at a density of 1×10^4 cells per well in 48-well plates in 300 μL of growth media. At twenty-four hours after seeding, the media was aspirated and cells were exposed to the DiD-labeled LNPs at the indicated final lipid concentrations. Cells were washed by PBS(-), trypsinized, and diluted with growth media at the indicated times after exposure. The cell suspension was transferred to 1.5 mL tubes and centrifuged at 100 g for 4 min. One mL of D-PBS(-) was added to each tube to resuspend the cells, followed by another round of centrifugation and resuspension using 1 mL of FACS buffer. The samples were measured using a Gallios Flow Cytometer (Beckman Coulter, Inc.) The DiD was excited with a red laser (638 nm), with detection using a 660/10 nm bandpass filter.

Annexin V Apoptosis Assay Cells were seeded at a density of 2×10^4 cells per well in 12-well plates in 1 mL of growth media. At approximately 90% confluency, the media was removed by aspiration and cells were exposed to the LNPs at the indicated final lipid concentrations. Attached cells were washed with D-PBS(-), trypsinized, and combined with floating cells. The cells were centrifuged at 400 g for 4 min and resuspended in 1 mL of D-PBS(-). A MEBCYTO Apoptosis Kit (MBL, Japan) was used for Annexin V labeling in accordance with the manufacturer's protocol. Cell suspension was centrifugated again and resuspended using 85 μL of binding buffer followed by the addition of 10 μL of Annexin V-FITC and 5 μL of propidium iodide (PI). The samples were left to incubate at room temperature for 15 min in the dark. After the incubation, 400 μL of binding buffer was added to the samples. The samples were measured using Gallios Flow Cytometer (Beckman Coulter, Inc.) The fluorophores were excited with a blue laser (488 nm) and were detected using 525/40 nm and 620/30 nm bandpass filters for FITC and PI, respectively.

Statistical Analyses Experiments were repeated on different cell passages in duplicates. Results are expressed as the mean±SD. Statistical comparisons between two groups were evaluated by the Student's *t*-test. The 50% effective dose (ED_{50}) was determined by the lipid concentration which corresponds to a 50% cell viability.

RESULTS

Characterization of LNPs As previously reported,[8] the LNP used in this study, YSK05-LNP, forms a spherical vesicle of YSK05 (Fig. 1), cholesterol, and PEG that surrounds siRNA as its designated cargo. Due to the cationic nature of YSK05 at an acidic pH, mixing it with the negatively charged siRNAs under acidic condition greatly aids in the formulation of these spherical vesicles due to ionic attractions, resulting in the formation of stable LNPs with diameters in the 80-120 nm range, a low polydispersity index (PDI) of 0.2 to 0.08, and a near neutral ζ-potential of 0±5 mV (Table 1). In this study, we used two types of PEG-lipids (PEG-DMG and PEG-DSG) to prepare 2 types of YSK05-LNPs (PEG-DMG YSK05-LNPs and PEG-DSG YSK05-LNPs, respectively). These PEG-lipids differ mainly in the length of hydrophobic scaffolds which confers a different stability in serum/media and different cellular uptake rate.[8,13,14] Due to these differences, these two different PEG-lipids were used to assess the toxicity of the system based on the different uptake rates to determine the location of the toxicity. Despite having different chain lengths, the resulting YSK05-LNPs measurements were consistent in all parameters (diameter, PdI and ζ-potential) as can be seen in Table 1. Although the addition of extra substances would be expected to alter these readings, their effect was minimal in our case, as seen by the negligible difference between the DiD-labeled and unlabeled YSK05-LNPs (Table 1).

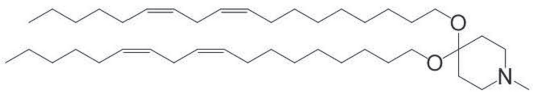

Fig. 1. Chemical Structure of the pH-Sensitive Cationic Lipids, YSK05, Used in this Study.

The YSK05 contains a tertiary amino group that can be protonated under a weakly acidic pH but not at a neutral pH.

Table 1. Summary of the Diameters, Polydispersity Index (PdI), and ζ-Potentials for the Various YSK05-LNPs

YSK05-LNPs	diameter (nm)	PdI	ζ-potential (mV)
PEG-DMG	72.7 ± 1.8	0.13 ± 0.02	+6.3 ± 2.1
PEG-DSG	78.2 ± 2.2	0.1 ± 0.04	+5.3 ± 0.3
PEG-DMG (DiD-labeled)	75.8 ± 0.6	0.21 ± 0.03	+6.5 ±2.4
PEG-DSG (DiD-labeled)	75.1 ± 1.7	0.15 ± 0.04	+5.4 ±2.2

All values are presented as the mean±SD, n=3.

Table 2. Average ED_{50} of YSK05-LNPs with Two Different PEG Modifications (PEG-DMG and PEG-DSG) and YSK05 in Its Free form (Free YSK05) After 24, 48, and 72 h of Exposure to A375 Melanoma Cell Lines

ED_{50} (μM) in A375	24 h	48 h	72 h
PEG-DMG YSK05-LNPs	90	60	7
PEG-DSG YSK05-LNPs	60	50	4
Free YSK05	>160	>160	4

Results obtained from Fig. 2A-C.

Table 3. Average ED_{50} of YSK05-LNPs with Two Different PEG Modifications (PEG-DMG and PEG-DSG) and YSK05 in Its Free form (Free YSK05) After 24, 48, and 72 h of Exposure to A375-SM Melanoma Cell Lines

ED_{50} (μM) in A375-SM	24 h	48 h	72 h
PEG-DMG YSK05-LNPs	90	15	5
PEG-DSG YSK05-LNPs	60	10	3
Free YSK05	>160	>160	3

Results obtained from Fig. 2D-F.

Cell Viability In order to assess the extent of toxicity caused by YSK05-LNPs on both A375 and A375-SM cell lines, serially diluted concentrations of YSK05-LNPs and free YSK05 were used to assess the dose-dependency aspect of this toxicity. The time-dependency aspect of this toxicity was assessed based on measurements at three selected time points, 24, 48, and 72 h.

The results of the cell viability assay for the A375 cell line in Fig. 2 (A, B, C) showcase the dose-dependent and time-dependent toxicity of the YSK05-LNPs while free YSK05 exhibited only a time-dependent toxicity. Starting at 24 h, concentrations of up to 40 μM of both YSK05-LNPs did not cause a significant decrease in cell viability, with as much as 80% viability being retained. On the other hand, concentrations above 40 μM showed a sharp decline in viability down to 20% with an 50% effective dose (ED_{50}) of 60-90 μM. Free YSK05 did not cause any decline in cell viability as it was retained at above 80% at all concentrations. At 48 hours, concentrations up to 40 μM again did not cause a significant decline in cell viability, but unlike 24 h, cell viability was retained at 60%. Furthermore, concentrations above 40 μM showed a sharper decline in cell viability in comparison to 24 h, decreasing below 20% with an ED_{50} of 50-60 μM. Again, free YSK05 did not cause any decline in viability below 80% at all concentrations. After 72 h of exposure, only low concentrations of both YSK05-LNPs up to 2.5 μM and 5 μM, respectively, maintained high (80%) cell viability. Concentrations above these two values resulted in a sharp decline in viability (≤20%) for each LNP, respectively, with an ED_{50} of 4-7 μM. Furthermore, free YSK05 exhibited a consistent pattern to PEG-DSG YSK05-LNPs, producing a sharp decline in viability starting at concentrations of 2.5 μM with an ED_{50} of 4 μM.

The results of cell viability assays for the A375-SM cell line in Fig. 2D-F showcase a similar dose-dependent and time-dependent toxicity for the YSK05-LNPs, while free YSK05 exhibited a time-dependent toxicity only. Similar to the A375 cells, 24 h exposure of both YSK05-LNPs at concentrations above 40 μM resulted in toxicity with a similar ED_{50} of 60-90 μM. Similarly, for free YSK05, cell viability was higher than 80% at all concentrations. By 48 h, however, exposure to both YSK05-LNPs caused a gradient decline in viability for A375-SM cells with an ED_{50} of 10-15 μM, which is in contrast to the sharp decline at a specific concentration (>40 μM) seen in A375 cells. As for free YSK05 exposure, a cell viability above 60% was retained at all concentrations, which is lower than the 80% viability of A375 cells. Lastly, a 72 h exposure resulted in a sharper decline in viability from as low as 2.5 μM and 5 μM for the PEG-DSG YSK05-LNPs and PEG-DMG YSK05-LNPs, respectively, decreasing directly from 80% to 20% after those two values with an ED_{50} of 3-5 μM. Again, similar to A375, the resulted for free YSK05 were similar to those for the PEG-DSG YSK05-LNPs, with a sharp decline from as early as 2.5 μM with an ED_{50} of 3 μM. In summary, the toxicity profiles at 24 and 72 h were similar for both cells, but differed at 48 h. All ED_{50} values are summarized in Tables 2 and 3.

Cellular Uptake Cellular uptake is an important factor in the functionality and dosage determination of LNPs.[15-18] Given that this toxicity is dose-dependent despite the fact that two different PEGylations with different uptake rates were used,[8,13,14] the cellular uptake for these cells becomes an important issue. Both cell lines were exposed to low concentrations of LNPs (1.25, 5, and 20 μM) to avoid cell death, while the uptake rate was measured at 3, 24, and 48 h to compare these values against cell viability.

For the A375 cell line, PEG-DMG YSK05-LNPs were taken up rapidly by cells at 3 h and this uptake remained constant up to 48 h. The PEG-DSG YSK05-LNPs were not taken by cells as efficiently as the PEG-DMG YSK05-LNPs and the uptake was 100-fold lower but remained constant up to 48 h. The exact same pattern was seen in the case of the A375-SM cell line, i.e., a high uptake of the PEG-DMG YSK05-LNPs and a low uptake of the PEG-DSG YSK05-LNPs. These results confirm that the rate of uptake exhibited by these cells was not an anomaly, in that the rate of uptake for particles that had different PEGylation were similar. All of the results are illustrated in Fig. 3.

Annexin V Assay Since a knowledge of the type of cell death is essential in terms of understanding mechanisms of toxicity,[19-25] an Annexin V apoptosis assay was performed. This assay consists of an FITC-conjugated Annexin V (AV) protein that binds phosphatidylserine, a marker of apoptosis, and propidium iodide (PI), a DNA-binding dye which functions as a marker of cell wall integrity loss due to necrosis.

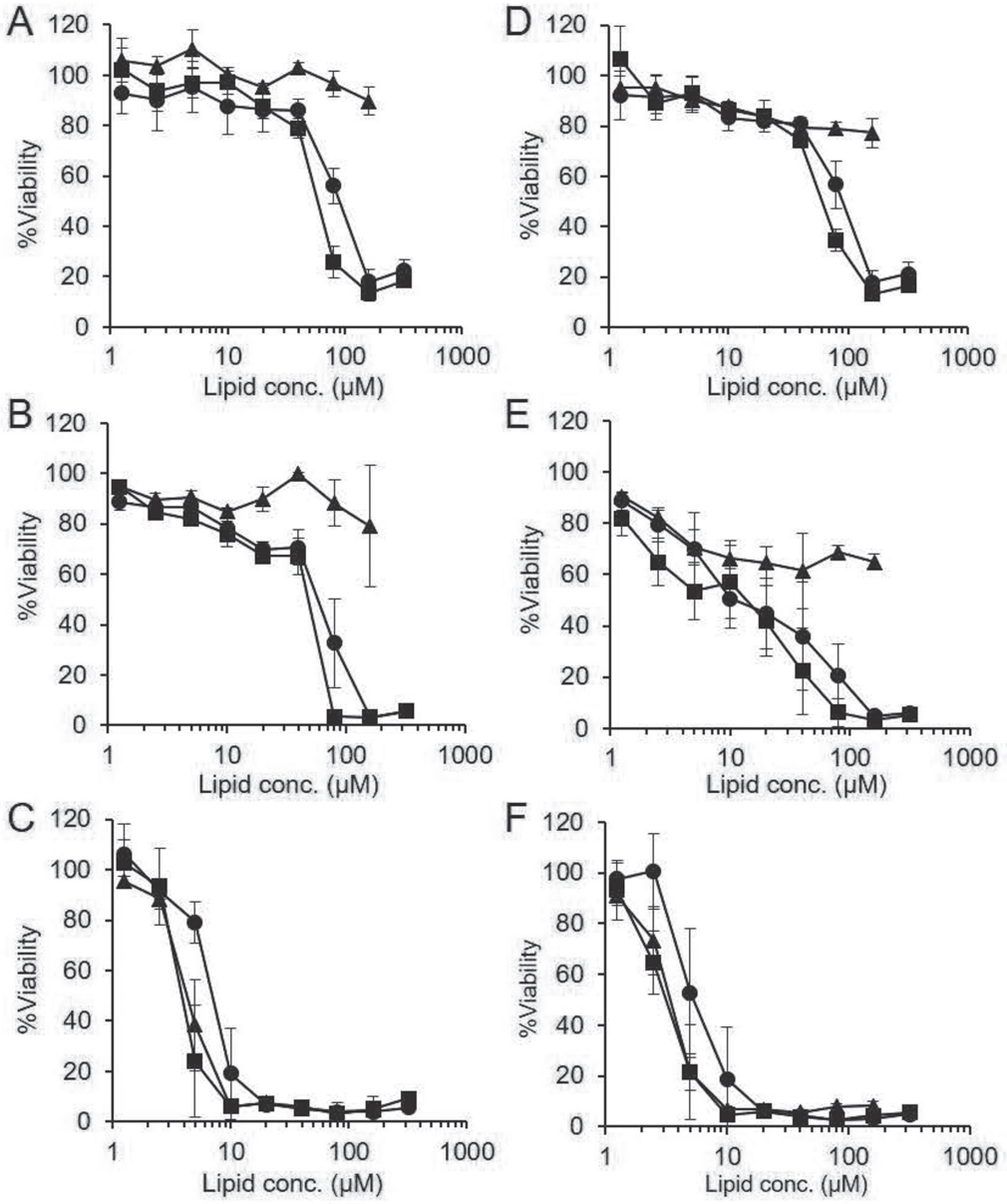

Fig. 2. WST-8 Cell Viability Assay of A375 (A-C) and A375-SM (D-F) Melanoma Cell Lines After 24 (A, D), 48 (B, E), and 72 (C, F) h of Exposure to PEG-DSG YSK05-LNPs (■), PEG-DMG YSK05-LNPs (●), and Free YSK05 (▲).

Results are presented as the mean ±SD. n=3.

In this case, however, to avoid screening cells during the late stages of apoptosis, a short time frame of 6, 12, and 24 h was selected. The corresponding LNP concentrations to cause significant toxicity at this short time were 80 μM and higher. Hence, both the highest concentration used (320 μM) and the start of viability decline (80 μM) in both cell lines for both LNPs was selected.

As seen in Fig. 4A-C, the majority of the A375 cells were double stained with both AV and PI, an indication of necrosis or late apoptosis for both YSK05-LNPs (PEG-DMG and PEG-DSG) at both concentrations (320 μM and 80 μM) and the three time points (6, 12, and 24 h). Some staining with PI was observed for both LNPs at both concentrations and all time points. However, for AV, essentially negligible staining was observed at 24 h. The ratio of necrotic cells to living cells was higher at 320 μM than at 80 μM and it increased linearly, as illustrated in Fig. 5A. For the A375-SM cells, a similar pattern of double staining was evident, but the staining ratio of PI was higher at 24 h, as shown in Fig. 4D-F. Again, the ratio of necrotic cells to living cells continued to increase linearly, as illustrated in Fig. 5. These results confirm that type of necrotic cell death had occurred.

DISCUSSION

LNPs differ from typical nanoparticles in their lack of reactivity due to the fact that they contain physiologically-compatible stable lipids and are large sized.[4,26] This makes them a nanoparticle of choice for use in drug delivery systems. YSK05-LNPs is a stable, non-toxic siRNA-carrying LNP that can be used in the therapeutic targeting of cancer cells both *in vivo* and *in vitro*.[6–8] However, this non-toxic YSK05-LNP showed a surprising level toxicity towards A375 (early stage) and A375-SM (late stage) melanoma cell lines. The

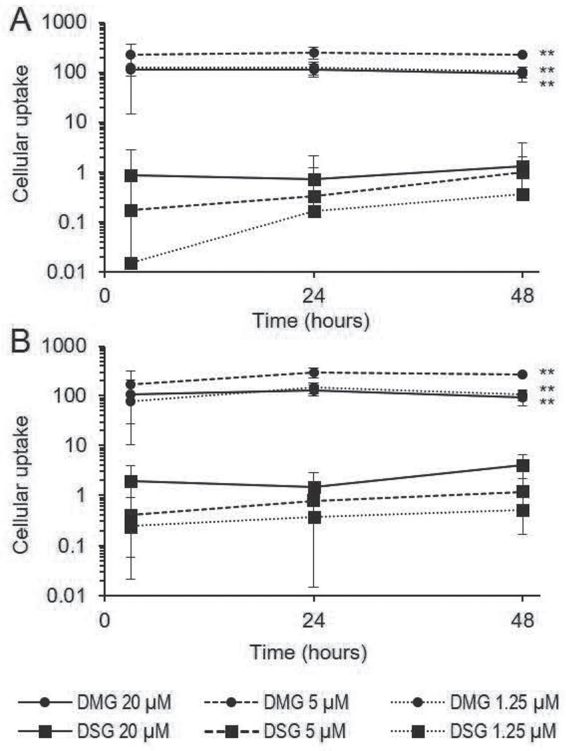

Fig. 3. Cellular Uptake of the PEG-DMG YSK05-LNPs and the PEG-DSG YSK05-LNPs for A375 (A) and A375-SM (B) Melanoma Cell Lines.

Multiple concentrations (1.25, 5, and 20 μM) and time points (3, 24, and 48 h) are shown. Results are presented as the mean ±SD. n=3. $^{**}P<0.01$ (vs. the concentration of each of the PEG-DSG YSK05-LNPs).

construction of a gradient toxicity curve is essential for developing a further understanding of this toxicity. Our data in Fig. 2 indicates that the dose-dependent toxicity caused by YSK05-LNPS, as both PEG-DMG YSK05-LNPs and PEG-DSG YSK05-LNPs caused similar toxicities at higher concentrations (80 μM and higher) while at lower concentrations, no significant toxicity was observed. This typical toxicity pattern[15,16,18,22,25,27-29] was similar for both A375 and A375-SM cell lines. However, a longer exposure time (up to 72 h) allowed lower concentrations (<80 μM) to overcome this dividing point and to trigger toxicity as well (Figs. 2C and F). This was true for both PEGylation for both cell lines. This is better displayed if the results are examined as a function of time; a shorter time exposure resulted in generally less toxicity while a longer exposure time resulted in more toxicity. This demonstrates the importance of time as a factor in initiating this toxicity (Fig. 2). Previously reported results showed a significant difference in uptake between both PEGylations (PEG-DMG and PEG-DSG) that were used.[7,8,13,14] This is mainly due to difference in length of the hydrophobic chains between both the PEG-DMG (C_{14}) and PEG-DSG (C_{18}). PEG originally functions as a protective shield to prevent interactions between blood, media, or cell surface components and this permits the LNP to have a higher circulation time *in vivo* and a higher LNP integrity both *in vitro* and *in vivo*.[13,14] This was further confirmed for YSK05-LNPs by the difference in the IC_{50} value for GL4 gene silencing capabilities. Where the DMG-modified YSK05-LNPs possess an IC_{50} value of 2 nM siRNA, and DSG-modified YSK05-LNPs possess an IC_{50} value of 12 nM siRNA in HeLa human cervical epithelioid carcinoma cell line.[8] Converting these values to μM of lipid according to the YSK05 preparation protocol, these values correspond to 53.4 μM lipid and 320 μM lipid. The fact that similar toxicity results were found when different PEGylations were used suggests that the differences between uptake and toxicity are not relevant for systems such as these. In order to confirm this hypothesis, the rate of uptake for both PEGs on both cell lines was measured. As expected, the rate of uptake for each PEG were different, as seen in Fig. 3.

Comparing the difference in uptake rate and the similar toxicities during a 48 h exposure confirms that the difference between uptake and dose-dependent toxicity are irrelevant. This raises the question of the location where this toxicity is triggered, i.e., intracellular or extracellular? When examining the intercellular conditions, we observed a 100-fold difference in uptake between those two PEGs. This translates into a 100-fold difference in dosage being delivered to cells, which should result in different toxicities. However, the above data does show no difference between both PEGs at this period, on the contrary, dose-dependency is clearly a component of this toxicity. The possibility that a 100-fold difference in dosage could cause a similar dose-dependent intracellular toxicity is low. On the other hand, regarding extracellular conditions, previous studies indicate that not all of the YSK05-LNPs present in media are fully internalized by cells,[8] only 5%-30% of total PEG-DMG YSK05-LNPs is internalized. This finding indicates that a 100-fold difference in uptake represents only a 100-fold difference in the fraction of the YSK05-LNPs present in the media, which further indicates that the difference in concentration between both YSK05-LNPs in the media is only 30% at a maximum during the exposure time. The possibility that similar amounts of YSK05-LNPs in the media triggering similar dose-dependent extracellular toxicity is high.

Another important aspect to be considered is the effect of YSK05 itself. The question arises as to whether it causes toxicity in its free form or is it necessary to be incorporated into LNPs to trigger this toxicity. This led to investigating the toxicity of YSK05 in its free form. As seen in Fig. 2, lower concentrations of free YSK05 were found to produce toxicity in both cell lines, but only after a longer exposure time. Even at higher concentrations where YSK05-LNPs caused toxicity (80 μM and higher), free YSK05 showed no toxicity. This suggests a lack of dose-dependency for the toxicity of free YSK05, which is present in the YSK05-LNPs. Furthermore, considering the fact that both free YSK05 and YSK05-LNPs can trigger similar toxicities after 72 h of exposure, this suggests that this this time-dependent toxicity is similar for both preparations. These differences and similarities between free YSK05 (time-dependency) and YSK05-LNPs (dose- and time-dependency) can be interpreted as representing two different modes of toxicity: 1) a fast-acting, acute toxicity resulting from high concentrations of the YSK05-LNP formulation, and 2) a slow-acting toxicity resulting from different concentrations of both YSK05-LNPs and free YSK05. It should be noted that one concern regarding the time-dependent toxicity is the effect of pH on the YSK05. Since the *in vitro* systems lack the ability to clear waste products unlike *in vivo* systems, the accumulation of metabolic byproducts in the media can decrease the pH even when buffers are used. The change of pH from physiological conditions to acidic conditions would result in the surface charge of the YSK05 being

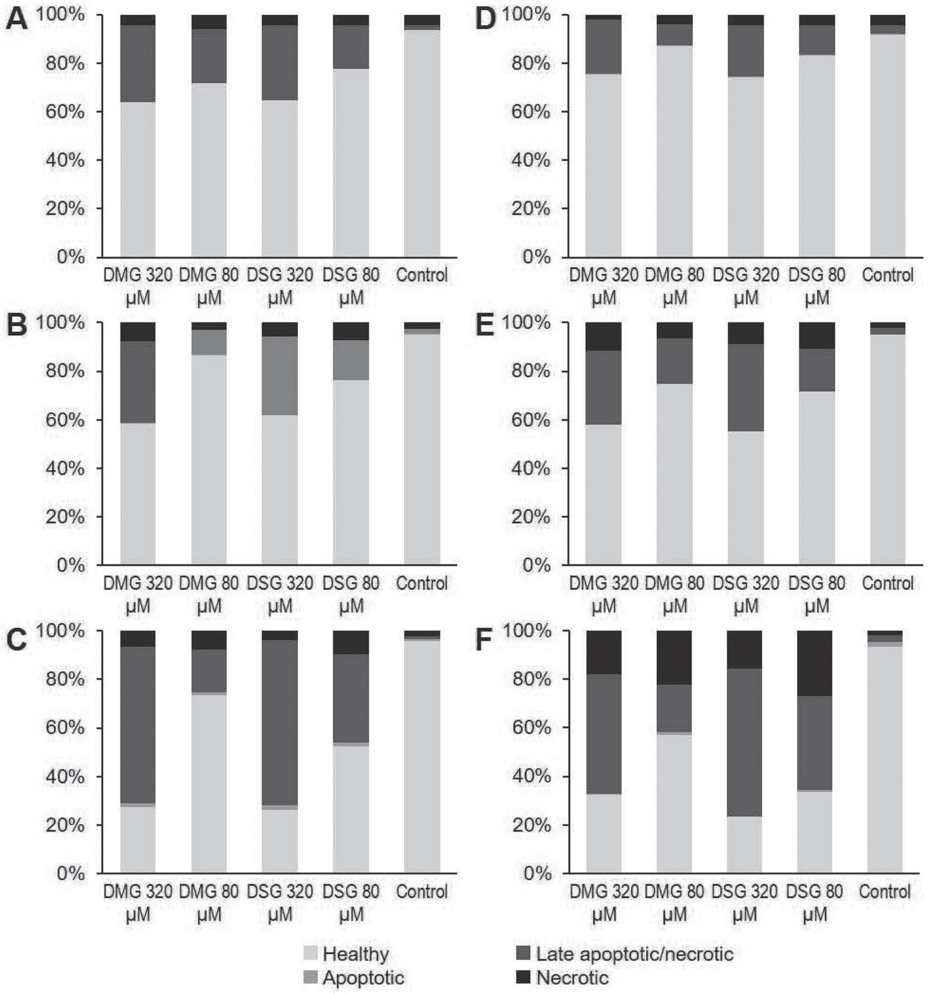

Fig. 4. Annexin V Assay of A375 (A-C) and A375-SM (D-F) Melanoma Cell Lines 6 (A, D), 24 (B, E), and 48 (C, F) h After Treatment with PEG-DMG YSK05-LNPs (DMG) and PEG-DSG YSK05-LNPs (DSG) at Concentrations of 320 and 80 μM Lipid.

Results are divided into healthy (no staining), apoptotic (AV staining), late apoptosis or necrosis (double AV and PI staining), and necrotic (PI staining).

altered to have cationic characteristics, due to its pH-sensitive nature. However, this requires the media to reach a pH lower than the pKa of the YSK05, which is 6.5,[30] to alter its charge. This pH would result in a noticeable change in the color of phenol red in the media, which takes on a yellow color when the pH reaches 6.8 and below. Visible observations made during the experiments resulted in only an orange color but never a yellow color. To fully challenge the pH hypothesis, cells were treated with YSK05-LNPs under conditions where a pH of 6.8 and a pH of 7.8 were maintained using appropriate buffers (MES and HEPES buffers, respectively). However, no difference in toxicity was observed for either of these pH conditions and similar toxicity patterns were observed (Fig. S2), suggesting that the observed time-dependent toxicity is independent of the change in pH.

Determining the type of cell death is a crucial issue in understanding toxicity mechanisms.[19-25] As seen in our data (Fig. 4), cell death appears to be by necrosis, as evidenced by the fact that double staining with both AV and PI was dominant, even at 6 h. The linear increase in necrotic to healthy cells (Fig. 5) fits perfectly with the toxicity curve, which also serves as a confirmation for the actual initiation of toxicity, thus ruling out any suspicion that this double staining would be dur to late apoptosis. When comparing these results to other nanotoxicity studies, many cases of inorganic nanoparticles inducing this type of toxicity can be found for silver,[27] silica,[23] carbon[22] but not lipids.[31] The toxicity of most nanoparticles can be attributed to the reactive properties of these nanoparticles. In the case of metallic nanoparticles, the high redox reactivity of the metals contained in them generates reactive oxygen species after being internalized, which results in either apoptosis or necrosis.[24,27,29,32] However, inorganic nanoparticles either interact with pro-apoptotic signaling pathways[23] or cause cell cycle arrest resulting in necrosis,[22] and also need to be internalized. This highlights an important aspect of nanotoxicity, namely that internalization is required to trigger intracellular toxicity. Which contrasts with our findings that point to an extracellular interaction between the YSK05-LNPs and the cell surface to trigger toxicity. Unfortunately, this interaction remains undetermined at this point. The only similar cell surface interactions that result in toxicity, are either pure metal nanoparticles,[33] which interact with plasma membranes before being internalized and cause necrosis, or viruses,[34] which bind to membrane signaling receptors and cause apoptosis. Although we can speculate that the YSK05-LNPs interact with a membrane protein or with a structure unique

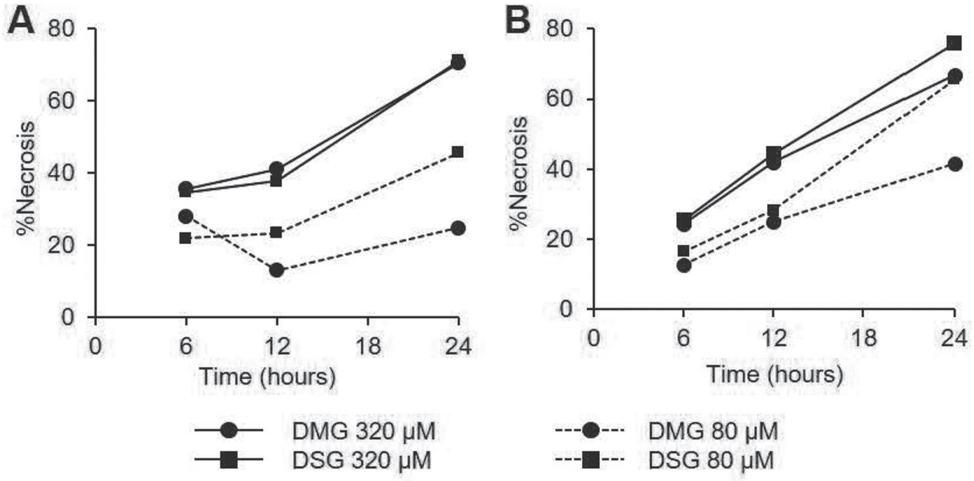

Fig. 5. Ratio Necrosis for A375 (A) and A375-SM (B) Melanoma Cell Lines After Exposure of the PEG-DMG YSK05-LNPs (DMG) and the PEG-DSG YSK05-LNPs (DSG) at Concentrations of 80 and 320 μM over 6, 12, and 24 h.

Ratios are calculated from Annexin V FACS as a sum of PI stained cells and AV and PI stained cells.

to these melanoma cell lines and this interaction either results in a lethal structure or initiates a cascade of interactions that results in necrotic death, the detailed mechanism for the interaction between the YSK05-LNPs and cell surface should be clarified by further examinations.

In conclusion, we report herein that A375 and A375-SM melanoma cell lines underwent an unexpected toxicity when exposed to non-toxic YSK05-LNPs. This toxicity appears to be extracellularly induced by an interaction between the LNPs and the cell surface and is both dose-dependent and time-dependent. The overall process appears to involve two modes of action: a fast-acting toxicity due to the YSK05-LNPs formulation, and a slow acting toxicity due to YSK05 itself, regardless of whether it is intimately involved in the LNP formation or in the free form. Annexin V assays confirmed that the type of cell death to be necrosis, as evidenced by the loss of cell membrane integrity and double labeling with Annexin V and Propidium Iodide. Further detailed studies will clearly be needed to completely understand the mechanisms involved in this process and the extent of this toxicity.

Future perspectives regarding these findings revolve around YSK05 itself. Melanomas are a devastating type of skin cancer with a low survival rate.[2] If YSK05 in the free form or as a component of an LNP could prove to be toxic towards other types of melanoma cells and/or skin cancer types, it could be a promising potential chemotherapeutic drug either intravenously or as a topical medication after the investigating its toxicity against normal skin cells.

Acknowledgments

This work was supported by the Special Education and Research Expenses from the Ministry of Education, Culture, Sports, Science and Technology. We would like to thank Dr. I.J. Fidler for providing A375SM cells, the super-metastatic human malignant melanoma cell line. The authors also wish to thank Dr. Milton S. Feather for his helpful advice in preparing the English manuscript.

Conflict of interest The authors who have taken part in this study declare that they have nothing to disclose regarding funding or conflict of interest with respect to the findings that appear in this manuscript.

REFERENCES

1) Gray-Schopfer V, Wellbrock C, Marais R. Melanoma biology and new targeted therapy. *Nature*, **445**, 851–857 (2007).
2) Balch CM, *et al*. Prognostic factors analysis of 17,600 melanoma patients: validation of the American Joint Committee on Cancer melanoma staging system. *J. Clin. Oncol.*, **19**, 3622–3634 (2001).
3) DeSantis CE, *et al*. Cancer treatment and survivorship statistics, 2014. *CA Cancer J. Clin.*, **64**, 252–271 (2014).
4) Sato Y, *et al*. Innovative Technologies in Nanomedicines: From Passive Targeting to Active Targeting/From Controlled Pharmacokinetics to Controlled Intracellular Pharmacokinetics. *Macromol. Biosci.*, **17** (2017).
5) Hoy SM. Patisiran: First Global Approval. *Drugs*, **78**, 1625–1631 (2018).
6) Matsui H, *et al*. Size-dependent specific targeting and efficient gene silencing in peritoneal macrophages using a pH-sensitive cationic liposomal siRNA carrier. *Int. J. Pharm.*, **495**, 171–178 (2015).
7) Sakurai Y, *et al*. Gene silencing via RNAi and siRNA quantification in tumor tissue using MEND, a liposomal siRNA delivery system. *Mol. Ther.*, **21**, 1195–1203 (2013).
8) Sato Y, *et al*. A pH-sensitive cationic lipid facilitates the delivery of liposomal siRNA and gene silencing activity *in vitro* and *in vivo*. *J. Control. Release*, **163**, 267–276 (2012).
9) Tamaru M, *et al*. An apolipoprotein E modified liposomal nanoparticle: ligand dependent efficiency as a siRNA delivery carrier for mouse-derived brain endothelial cells. *Int. J. Pharm.*, **465**, 77–82 (2014).
10) Watanabe T, *et al*. In vivo therapeutic potential of Dicer-hunting siRNAs targeting infectious hepatitis C virus. *Sci. Rep.*, **4**, 4750 (2014).
11) Ohga N, *et al*. Heterogeneity of tumor endothelial cells: comparison between tumor endothelial cells isolated from high- and low-metastatic tumors. *Am. J. Pathol.*, **180**, 1294–1307 (2012).
12) Maishi N, *et al*. Tumour endothelial cells in high metastatic tumours promote metastasis via epigenetic dysregulation of biglycan. *Sci. Rep.*, **6**, 28039 (2016).
13) Chen S, *et al*. Influence of particle size on the *in vivo* potency of lipid nanoparticle formulations of siRNA. *J. Control. Release*, **235**, 236–244 (2016).
14) Zhu X, *et al*. Surface De-PEGylation Controls Nanoparticle-Mediated siRNA Delivery In Vitro and In Vivo. *Theranostics*, **7**, 1990–2002 (2017).

15) Gliga AR, *et al*. Size-dependent cytotoxicity of silver nanoparticles in human lung cells: the role of cellular uptake, agglomeration and Ag release. *Part. Fibre Toxicol.*, **11**, 11 (2014).
16) Poulin P, Burczynski FJ, Haddad S. The Role of Extracellular Binding Proteins in the Cellular Uptake of Drugs: Impact on Quantitative In Vitro-to-In Vivo Extrapolations of Toxicity and Efficacy in Physiologically Based Pharmacokinetic-Pharmacodynamic Research. *J. Pharm. Sci.*, **105**, 497–508 (2016).
17) Suzuki Y, Ishihara H. Structure, activity and uptake mechanism of siRNA-lipid nanoparticles with an asymmetric ionizable lipid. *Int. J. Pharm.*, **510**, 350–358 (2016).
18) Zhang P, *et al*. Cellular uptake and cytotoxicity of drug-peptide conjugates regulated by conjugation site. *Bioconjug. Chem.*, **24**, 604–613 (2013).
19) Crowley LC, *et al*. Dead Cert: Measuring Cell Death. *Cold Spring Harb. Protoc.*, **2016** (2016).
20) Crowley LC, *et al*. Quantitation of Apoptosis and Necrosis by Annexin V Binding, Propidium Iodide Uptake, and Flow Cytometry. *Cold Spring Harb. Protoc.*, **2016** (2016).
21) Ishibashi M, *et al*. Antiproliferative and apoptosis-inducing effects of lipophilic vitamins on human melanoma A375 cells *in vitro*. *Biol. Pharm. Bull.*, **35**, 10–17 (2012).
22) Kim JH, *et al*. Necrotic cell death caused by exposure to graphitic carbon-coated magnetic nanoparticles. *J. Biomed. Mater. Res. A*, **103**, 2875–2887 (2015).
23) Lee K, *et al*. Two distinct cellular pathways leading to endothelial cell cytotoxicity by silica nanoparticle size. *J. Nanobiotechnology*, **17**, 24 (2019).
24) Lee YH, *et al*. Cytotoxicity, oxidative stress, apoptosis and the autophagic effects of silver nanoparticles in mouse embryonic fibroblasts. *Biomaterials*, **35**, 4706–4715 (2014).
25) Zhang Y, *et al*. Evodiamine induces tumor cell death through different pathways: apoptosis and necrosis. *Acta Pharmacol. Sin.*, **25**, 83–89 (2004).
26) Zylberberg C, *et al*. Engineering liposomal nanoparticles for targeted gene therapy. *Gene Ther.*, **24**, 441–452 (2017).
27) Foldbjerg R, *et al*. PVP-coated silver nanoparticles and silver ions induce reactive oxygen species, apoptosis and necrosis in THP-1 monocytes. *Toxicol. Lett.*, **190**, 156–162 (2009).
28) Donaldson K, Poland CA. Nanotoxicity: challenging the myth of nano-specific toxicity. *Curr. Opin. Biotechnol.*, **24**, 724–734 (2013).
29) Kim J, Gilbert JL. In vitro cytotoxicity of galvanically coupled magnesium-titanium particles on human osteosarcoma SAOS2 cells: A potential cancer therapy. *J. Biomed. Mater. Res. B Appl. Biomater.*, **107**, 178–189 (2019).
30) Shobaki N, Sato Y, Harashima H. Mixing lipids to manipulate the ionization status of lipid nanoparticles for specific tissue targeting. *Int. J. Nanomedicine*, **13**, 8395–8410 (2018).
31) Tzankova V, *et al*. In vitro and *in vivo* toxicity evaluation of cationic PDMAEMA-PCL-PDMAEMA micelles as a carrier of curcumin. *Food Chem. Toxicol.*, **97**, 1–10 (2016).
32) Murphy MP. How mitochondria produce reactive oxygen species. *Biochem. J.*, **417**, 1–13 (2009).
33) Karlsson HL, *et al*. Cell membrane damage and protein interaction induced by copper containing nanoparticles--importance of the metal release process. *Toxicology*, **313**, 59–69 (2013).
34) Connolly JL, Barton ES, Dermody TS. Reovirus binding to cell surface sialic acid potentiates virus-induced apoptosis. *J. Virol.*, **75**, 4029–4039 (2001).